CONFERENCE PRE-PRINT

PROGRESS IN PLASMA-WALL INTERACTION MODELLING FOR EU-DEMO

D. MATVEEV*, C. BAUMANN, J. ROMAZANOV, S. BREZINSEK

Forschungszentrum Jülich GmbH, Institute of Fusion Energy and Nuclear Waste Management - Plasma Physics Juelich, Germany

*Email: d.matveev@fz-juelich.de

S. RATYNSKAIA, L. VIGNITCHOUK, P. TOLIAS, K. PASCHALIDIS

Space and Plasma Physics, KTH Royal Institute of Technology Stockholm, Sweden

D. TSKHAKAYA, M. KOMM, A. PODOLNÍK

Institute of Plasma Physics of the CAS Prague, Czech Republic

J. MOUGENOT, Y. CHARLES

University Sorbonne Paris-Nord, Process and Materials Sciences Laboratory Villetaneuse, France

E. HODILLE, J. DUFOUR

CEA IRFM

Saint Paul Lez Durance, France

U. VON TOUSSAINT, K. SCHMID

Max Planck Institute for Plasma Physics

Garching, Germany

F. GRANBERG, F. KPORHA

Department of Physics, University of Helsinki Helsinki, Finland

J. KOVAČIČ, S. COSTEA

Reactor Physics Department, Jožef Stefan Institute

Ljubljana, Slovenia

Abstract

Progress regarding plasma-wall interaction modelling for EU-DEMO is presented, which is a part of EUROfusion Theory and Advanced Simulation Coordination (E-TASC) activities that were established to advance the understanding and predictive capabilities for modelling of existing and future fusion devices using a modern advanced computing approach. The paper presents new results on erosion and re-deposition of tungsten studied with different assumptions on the far scrapeoff layer plasma parameters, the dust transport and inventory evolution for various starting locations and initial conditions, transient limiter melting during upward vertical displacement event accounting for spatial and temporal variation of the incoming heat flux, and studies on fuel retention in divertor monoblocks with trap creation and annealing model addressing neutron-induced defects, as well as an update on tritium self-sufficiency analysis.

1. INTRODUCTION

Plasma-wall interactions (PWI) are recognized as design- and safety-relevant aspects that can impose significant constraints on the operational space and availability of a reactor-scale fusion device such as DEMO. The "EUROfusion Theory and Advanced Simulation Coordination (E-TASC)" initiative launched in 2021 [1] includes PWI modelling for EU-DEMO as one of "Theory, Simulation, Verification and Validation (TSVV)" tasks [2] aiming at addressing high-priority issues along the roadmap to fusion energy with help of advanced simulations supported by high-performance computing (HPC). Following the initiation of TSVV projects, the integral approach to PWI modelling for EU-DEMO and first preliminary results were presented in [3].

The multilateral modelling effort is focused on assessment of safety-relevant information regarding plasma-facing components (PFC) in view of material erosion, dust production, and fuel inventory in steady-state plasma operation, as well as large-scale wall deformation during transient events. A set of powerful and validated computer codes provides the foundation for the modelling framework. In the core of the framework are such codes as ERO2.0 [4] for material erosion, transport and re-deposition studies under steady-state plasma conditions accounting for realistic 3D wall geometry; MIGRAINe [5] similarly for dust inventory evolution simulations; FESTIM [6] for tritium retention and permeation studies, both globally in 1D and locally on the monoblock level in 2D and 3D [7]; and MEMENTO [8, 9] for studies of transient material melting. Additional supporting activities include the work on advancement of physics understanding and numerical description for a variety of related processes and phenomena by means of particle-in-cell (PIC) simulations (BIT-1 [10] and SPICE [11]), in particular in view of thermionic electron emission effects [12], and Molecular Dynamics (MD) [13] and Monte-Carlo ion-material interaction codes [14], as well as efforts on optimization of codes' performance and standardization of codes' input and output workflow. Different aspects of PWI modelling addressed by the integral approach and corresponding code-code interactions are sketched in Fig. 1.

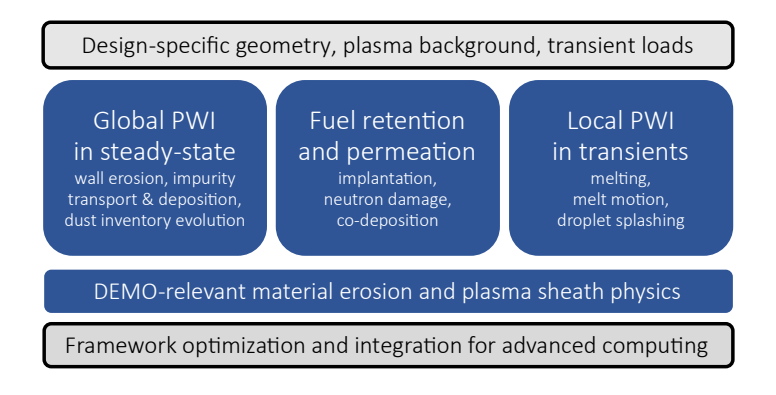


FIG. 1. A schematic diagram of different aspects of PWI modelling and their interaction within the integral approach. The upper layer corresponds to the essential data input. The middle layer represents the core of the TSVV task with three main research topics supported by auxiliary projects in view of underlying material and plasma sheath physics. The entire project is then oriented towards performance optimization in view of HPC and integration into the E-TASC infrastructure of advanced simulations (the bottom layer).

The paper reports on the progress of the project and is structured as follows. Section 2 describes the steady-state W erosion and re-deposition rates from ERO2.0 simulations. Section 3 covers the transport of dust particles injected from different locations using MIGRAINe. Section 4 elaborates the topic of fuel retention in divertor monoblocks and provides an update regarding tritium self-sufficiency analysis. Section 5 addresses transient melting simulations with MEMENTO for the case of vertical displacement events (VDEs). The paper concludes with a brief summary and an outlook on future research directions.

2. W EROSION AND RE-DEPOSITION IN STEADY-STATE PLASMA CONDITIONS

In the past, ERO2.0 was successfully applied to at that time hypothetical full-W ITER as a proxy for the EU-DEMO, and significant W sputtering by D charge-exchange neutrals (CXNs) in the main chamber was observed [15]. However, parameter studies assuming different fractions of seeded impurities in the background plasma identified that seeded impurities mostly dominate the erosion of both the divertor and the main chamber wall. The significance of this preliminary modelling approach was limited due to critical assumptions that had to be imposed, such as reliance on pure D plasma background without self-consistent feedback of seeding species on plasma parameters and the fact that seeding species were considered to be singly charged and constituting a given constant percentage of the plasma flux at all wall locations.

As a next step, the 3D CAD geometry of the EU-DEMO design and magnetic equilibrium for EU-DEMO Physics Baseline 2017 [16] were implemented in ERO2.0 with code-internal magnetic shadowing calculations for shaped first wall panels. The considered plasma scenario describes an ELM-free H-mode D plasma with argon (Ar) seeding and an expected fusion power of 2 GW, which was modelled with the narrow-grid version of SOLPS-ITER [17]. The fact that a narrow grid was used in SOLPS-ITER requires bridging large distances towards the main chamber wall in ERO2.0 (ranging between ~ 10 cm at the mid-plane up to about 80 cm above the outer divertor). A simple exponential decay of plasma parameters with uniform decay constant of 5 cm was therefore assumed. However, electron and ion temperatures were capped at some user-defined value. For

instance, the case of 2 eV was chosen in preliminary simulations reported in [3]. To study the impact of the far-SOL temperature profile on W erosion and migration, additional values of 5 eV and flat temperature profiles from the last existing flux surface in SOLPS-ITER towards the wall are presented here. In addition to different assumptions on the far-SOL temperature, newer ERO2.0 simulations also estimate the erosion by CXN based on kinetic energy distributions recorded at several poloidal locations across the machine [18, 19]. This advanced approach led to a reduction in the peak W erosion flux due to D CXN by a factor of 2.5. At the same time, however, additional W source locations emerged on the low-field and high-field side main chamber wall, where the mean CXN energy (used in former modelling) is below the sputtering threshold for W. Moreover, the refined ERO2.0 simulations use an updated boundary condition for the Mach number at the sheath entrance (normalization to the sound speed of an effective background, rather than to the individual Mach number of each species) to match the sheath boundary condition in the SOLPS-ITER background, thus increasing the consistency between the codes. Resulting erosion and deposition maps produced with the most recent version of the ERO2.0 code implementing above mentioned updates are shown in Fig. 2 for the three far-SOL temperature assumptions as discussed in the text.

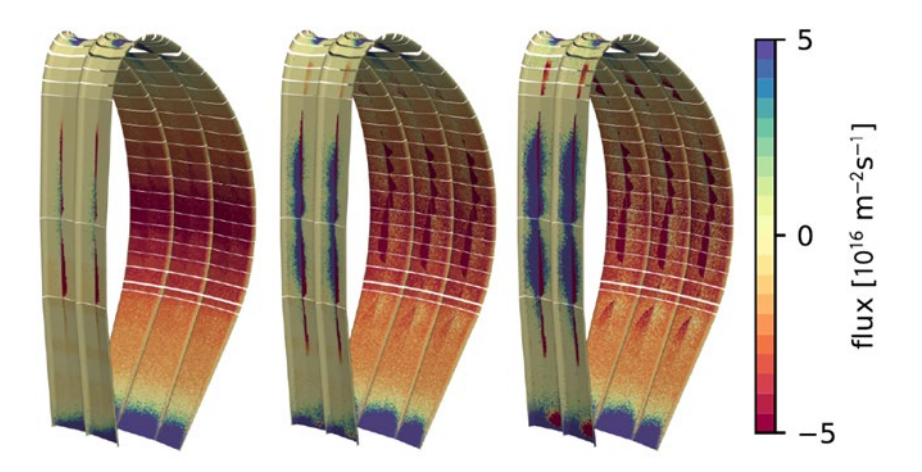


FIG. 2. Erosion and re-deposition maps obtained with the ERO2.0 code for the EU-DEMO under three different assumptions on the far-SOL temperature: an exponential decay with a 2 eV cut-off (left), same with a 5 eV cut-off (middle), and a flat temperature profile towards the wall from the last existing flux surface in the plasma grid of SOLPS (right).

Qualitatively, the dependence of W erosion and migration on the far-SOL temperature assumption for the EU-DEMO can be summarized as follows:

- (a) Tungsten main chamber erosion is dominated by D CXN for the coldest far-SOL temperature of 2 eV, but Ar sputtering becomes more dominant the higher the far-SOL temperature is and becomes dominant for the hottest temperatures considered here.
- (b) The ratio of the main chamber gross erosion to the divertor gross erosion ranges between 1/10 for the 2 eV case and 1/3 for the flat temperature profile case, indicating that main chamber erosion becomes more important the higher the temperature close to the wall.
- (c) There is a net W transport from the main chamber into the divertor, which slowly decreases with increasing far-SOL temperature, because ionization mean free paths in the main chamber are still rather long.

3. DUST TRANSPORT AND INVENTORY EVOLUTION SIMULATIONS

In the past, the transport of remobilized dust and the respective dust inventory evolution were simulated with the MIRGRAINe code for low-power ITER ramp-up discharges [5]. Different plasma parameters, dust sizes, and initial velocity distributions (assuming an inverse scaling between initial dust particle size and injection speed) were studied to address various dust mobilization scenarios. The simulations suggested that the injection speed has the strongest impact on the results. Similar conclusions were drawn from preliminary simulations for the EU-DEMO using the same wall geometry and steady-state plasma solution as in the ERO2.0 simulations described above [3].

In the meantime, the EU-DEMO simulations have been advanced by W dust trajectories calculations with and without accounting for the drag force due to bulk ion flows, accounting for seeded impurities in the plasma, and

considering predominant W re-deposition locations provided by ERO2.0 as re-mobilization sites. The space of initial conditions (particle size and velocity) expected for EU-DEMO is sampled by multiple individual deterministic trajectories, resulting in a final dataset of approximately 5.7 million particles, onto which numerical weights are applied as post-treatment to enforce various postulated initial statistical distributions. In total 14 dust injection sites (13 sites in the divertor region and one site on the top of the vessel, Fig. 3) have been selected based on ERO2.0 simulations of net W deposition areas for the 2 eV far-SOL case, as well as previous simulations of most likely dust accumulation sites. Fig. 3 shows examples of dust evaporation maps for these cases. The results confirm the conclusions from previous studies, namely that:

- (a) Vaporization is dominant for small grains.
- (b) Initial velocity has major impact on survival of particles of all sizes by governing how far they penetrate into hot and dense plasma regions.
- (c) Dust accumulates primarily in corner-like geometries at the bottom of the vessel such as divertor legs and boundaries between divertor baffles and the main chamber wall, with a skew towards the low-field side due to the centrifugal effect (Fig. 4).

Moreover, while ion drag has only a small effect on the shape of the spatial distribution of trajectory termination points in a single discharge (the average drag-induced shift is typically below 1° in toroidal angle), its cumulative impact on the total number of surviving particles – and hence on the characteristic inventory decay time – can still become significant over many consecutive discharges. As expected from first-principles scaling, ion drag has the strongest impact in scenarios where dust injection velocities are lowest.

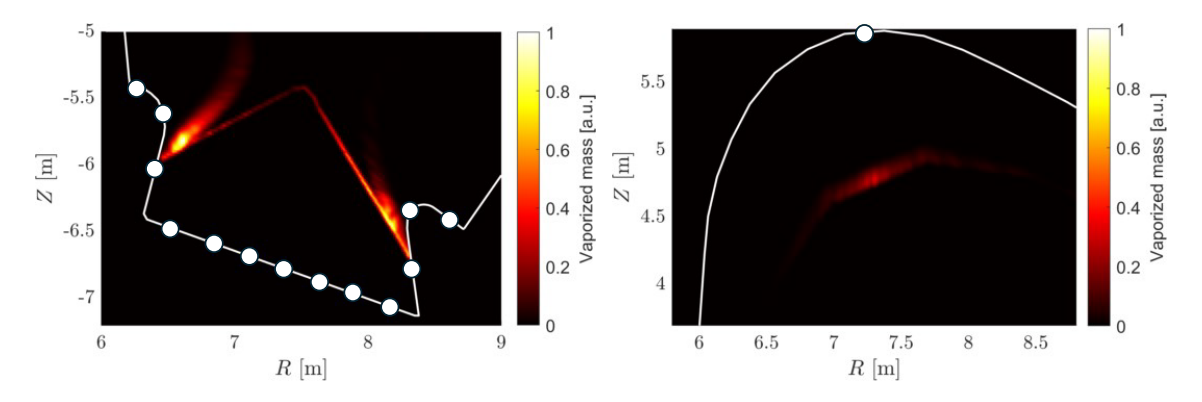


FIG. 3. Example of a simulated map of atomic W release due to dust vaporization during a single discharge, with ion drag active, for a modal initial dust radius of $10 \mu m$ and a maximal initial dust speed of $10 \mu m$. White circles denote the injection sites. Note that the imprint of the top injection site (right figure) is weaker compared to divertor injection sites (left figure) due its statistical weight representing only 1/14 of the total initial in-vessel dust mass (13 injection sites in the divertor and only one injection site at the top).

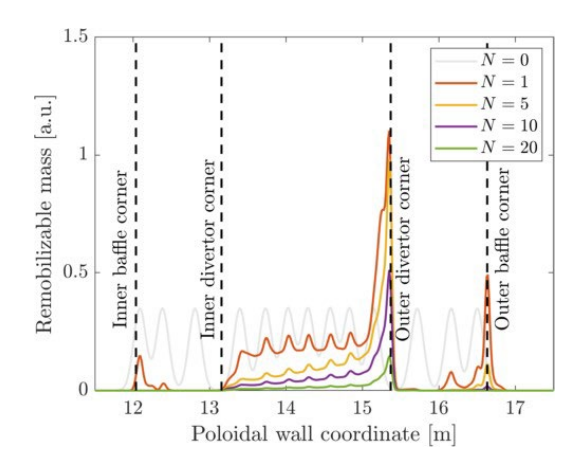


FIG. 4. Example of a simulated evolution of the spatial distribution of the re-mobilizable dust mass in the divertor region after N discharges, with ion drag activated, for a modal initial dust radius of 40 μ m and a maximal initial dust speed of 50 m/s. Each peak on the gray curve (N = 0) corresponds to one of the 13 divertor injection sites, which start with the same weight factor for the initial dust mass.

4. FUEL RETENTION

Using the EU-DEMO monoblock geometry [20] and the model of trap evolution including the trap creation from neutron damage and destruction by annealing [21], transient inventory simulations have been performed, accounting for the presence of the strong 2.05 eV trap. Fig. 5 shows the tritium concentration field in one monoblock after 200 thousand seconds of operation at different damage rates [22]. Results show that tritium concentration near the plasma-exposed surface increases by about 2 orders of magnitude due to the presence of a layer of strong neutron induced traps acting as a permeation barrier and a sink for mobile tritium. The total inventory after one effective full power year (EFPY) of operation increases by more than five orders of magnitude at the highest considered damaging rate of 100 displacements per atom (dpa) per EFPY [21, 22]. Moreover, tritium inventory is shown not to reach a point of saturation after one EFPY, highlighting the importance of kinetic models to describe the influence of neutron damage. In terms of tritium self-sufficiency, the wall retention reported earlier as potential showstopper [23] was re-evaluated with updated requirement on the maximum tritium wall-loss probability applying the state-of-the-art residence time model and concluding that wall retention constitutes only a small fraction of the total tritium throughput in the fuel cycle, thus not representing a self-sufficiency issue [24].

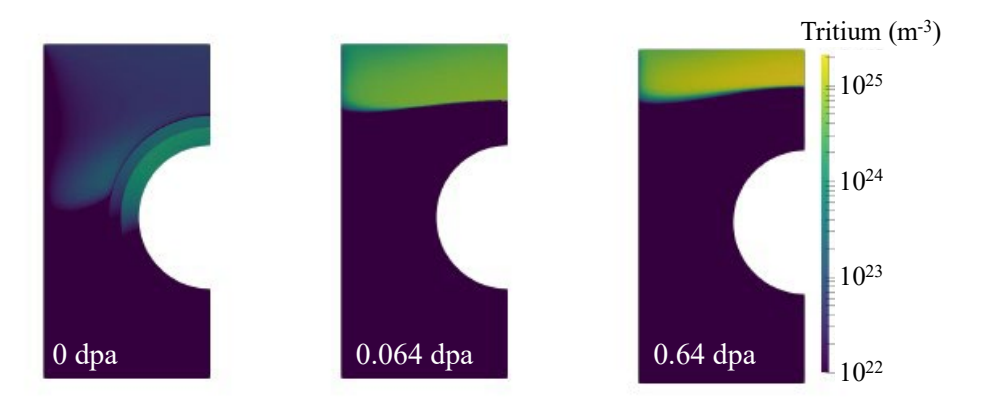


FIG. 5. Tritium retention field after 200,000 s of plasma exposure for different neutron fluxes (damage rates) compared to undamaged case (0 dpa): resulting damage up to 0.064 dpa (10 dpa/EFPY), and 0.64 dpa (100 dpa/EFPY) using the FESTIM code with the neutron trap damage creation and annealing model [21].

In addition to neutron damage effects, the role of helium is also addressed through cluster dynamics simulations using the FEniCS library [25]. It is shown that in order to reproduce the experimentally observed saturation of the bubble size growth with exposure fluence it is important to take into account the depletion of helium linked with bursting of helium bubbles. In particular, by explicitly considering dislocations as bubble nucleation sites, the bubble density increases and the predicted bubble radius is reduced.

5. TRANSIENT MELTING

Analysis by the EU-DEMO Central Team [26] revealed that the thermal quench (TQ) phase of vertical displacement events can result in surface heat loads relevant for melting, especially for the upper VDE (and the contact with the upper sacrificial limiter respectively) the maximal perpendicular heat load of 63 GW/m² is predicted, though for a very short duration of only 4 ms. The current quench (CQ) phase heat loads were estimated at about 2 GW/m² over ~100 ms duration. With the new data available, the predictions regarding limiter melting using new PFCFlux [27] input could be updated - now accounting for the fact that multiple points from the outer mid-plane can reach the same location on the wall and using spatially and temporally varying heat loads. Compared to the previous PFCFlux input, the maximum heat flux values are ~10 higher, reaching up to 28 GW/m² (assuming 50% conversion from all poloidal magnetic energy) or 5.6 GW/m² (assuming 10% conversion instead). Such intense heat loading results in surface temperatures reaching up to 7500 K (for 50% case) and 6500 K (for 10%). These temperatures are achieved because vapor shielding effects are not considered in the simulations. However, as pointed out in previous works, the melt depth is relatively robust against vapor shielding effects. Indeed, this is highlighted again by the fact that, although the heat flux between 50% and 10% cases was reduced by a factor of five, the characteristic instantaneous melt depth changes are within a factor of two. That said, it is important to note that neglecting vapor shielding significantly overestimates erosion damage, hence the deformation profiles are not reliable.

Even though the 10% conversion case is considered to be more realistic, severe damage occurring at 50% conversion is also presented as the worst-case scenario. Due to weak scaling of the escaping thermionic emission (TE) with the heat flux, the escaping TE in both scenarios is within $\sim 2-3$ MA/m², dominating over the halo current in the Lorentz force. Instantaneous melt pools are rather deep, reaching 0.3–0.5 mm in depth (Fig. 6). Melt in both scenarios is capable to reach the edge of the limiter and with melt characteristic corresponding to Weber number ~ 10 to 20 may be prone to splashing.

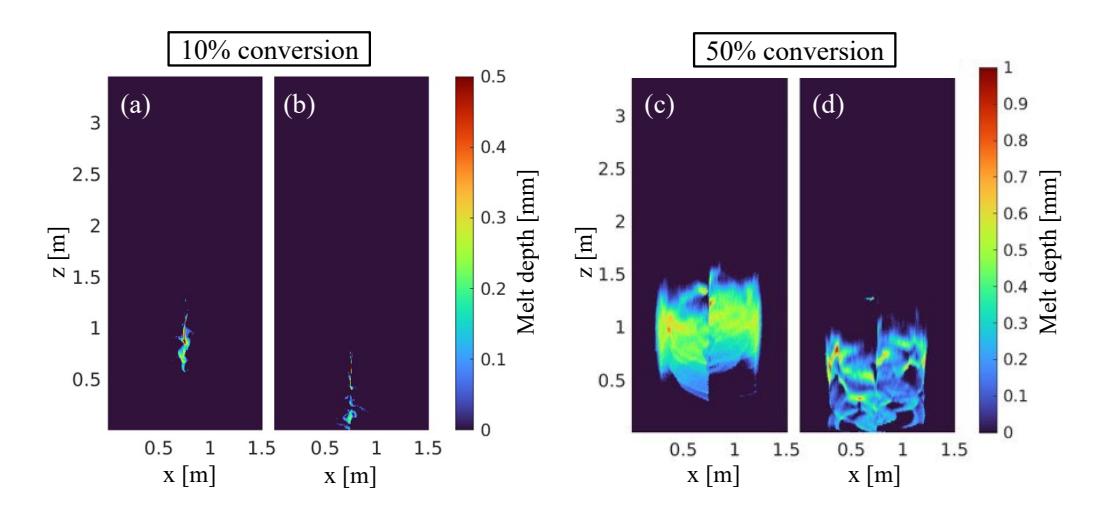


FIG. 6. Melt depth for the cases of 10% and 50% conversion of all poloidal magnetic energy. The melt depth is shown at two time instances, 40 ms (a, c) and 60 ms (b, d) after the start of loading.

SUMMARY AND OUTLOOK

The progress of the integral approach to PWI modelling for the EU-DEMO design was presented. It combines activities covering the design and safety relevant topics of wall materials erosion, transport and re-deposition in view of wall lifetime and fuel retention, problematics of dust re-mobilization and related inventory evolution, transient material damage in off-normal plasma events including assessment of likelihood of melt splashing and related droplet ejection.

In terms of wall life time simulations for steady state plasma operation, the critical aspects identified earlier [3] still remain actual. First of all, it concerns the need to bridge the gap between the "narrow" plasma grid and the wall using certain extrapolation assumptions, for which a consistent pre-processing pipeline had been developed in ERO2.0. The erosion of the outer wall dominated by CXN highlights the need for statistically accurate description of CXN impact characteristics (erosion dominated by the high energy tail of distribution). Improved assessment of these effects will be made as soon as a wide-grid SOLPS-ITER plasma solution extending to the wall becomes available for the new EU-DEMO design [28].

Global modelling of steady-state PWI on the tokamak scale with ERO2.0 is accompanied by dedicated local scale PWI studies towards better description of underlying particle reflection and sputtering models. This concerns better accuracy of differential yields for sputtering and reflection at low impact energies addressed by MD simulations, and assessment of deviations from classical Bohm-Chodura sheath models in the case of high density collisional divertor sheath addressed by PIC simulations.

Starting from W deposition locations simulated by the ERO2.0 code, particularly those in the divertor, and considering them as potential source of dust particles, dust transport and inventory evolution simulations with the dust dynamics code MIGRAINe were performed. Results include volumetric impurity source maps due to vaporization, overall dust inventory evolution and dust accumulation sites.

In view of fuel retention analysis for EU-DEMO the focus lies first of all on the effect of neutron damage on fuel inventory, permeation fluxes and overall tritium self-sufficiency for the plant operation. These topics are addressed in 1D for the large area of the first fall in the main chamber as well as considering W divertor monoblocks in 2D and 3D geometry, demonstrating the tremendous effect of bulk neutron damage on integral fuel retention.

Finally, the material damage during transients such as vertical displacement events (VDEs) is addressed. Material melting simulations have been enhanced with a state-of-the-art thermionic electron emission model derived from a large set of PIC simulations. New data for a spatially and temporally varying heat flux, obtained with the updated PFCFlux model, were employed for the assessment of the upper limiter damage. Simulations reveal formation of a melt pool up to about 0.5 mm depth. Under the considered conditions, the melt pool can reach the affected tile edge with possible splashing.

Further work is ongoing towards better framework integration for data exchange between codes, development of surrogate models for certain subsystems and validation on existing devices of relevance such as ASDEX Upgrade. This way the established modelling framework guides code development for unexplored DEMO-like conditions and supports the design of future machines, with the potential to enable iterative design-cycle integration.

ACKNOWLEDGEMENTS

This work has been carried out within the framework of the EUROfusion Consortium, funded by the European Union via the Euratom Research and Training Programme (Grant Agreement No 101052200 — EUROfusion). Views and opinions expressed are however those of the author(s) only and do not necessarily reflect those of the European Union or the European Commission. Neither the European Union nor the European Commission can be held responsible for them.

REFERENCES

- [1] LITAUDON, X. et al., EUROfusion-theory and advanced simulation coordination (E-TASC): programme and the role of high performance computing, Plasma Phys. Control. Fusion **64** 3 (2022) 034005.
- [2] JENKO, F., TOWARDS DIGITAL TWINS OF FUSION SYSTEMS: Achievements of the E-TASC initiative, (2025) this conference.
- [3] MATVEEV, D. et al., An integral approach to plasma-wall interaction modelling for EU-DEMO, Nucl. Fusion **64** 10 (2024) 106043.
- [4] ROMAZANOV, J. et al., Validation of the ERO2.0 code using W7-X and JET experiments and predictions for ITER operation, Nucl. Fusion 64 8 (2024) 086016.
- [5] VIGNITCHOUK, L., PASCHALIDIS, K., RATYNSKAIA, S., TOLIAS, P., PITTS, R.A., Remobilized dust dynamics and inventory evolution in ITER-like start-up plasmas, Plasma Phys. Control. Fusion **65** 1 (2023) 015014.
- [6] DELAPORTE-MATHURIN, R. et al., FESTIM: An open-source code for hydrogen transport simulations, International Journal of Hydrogen Energy 63 (2024) 786.
- [7] DELAPORTE-MATHURIN, R. et al., 3D effects on hydrogen transport in ITER-like monoblocks, Nucl. Fusion 64 2 (2024) 026003.
- [8] RATYNSKAIA, S. et al., Experiments and modelling on ASDEX Upgrade and WEST in support of tool development for tokamak reactor armour melting assessments, Nuclear Materials and Energy **33** (2022) 101303.
- [9] PASCHALIDIS, K., RATYNSKAIA, S., LUCCO CASTELLO, F., TOLIAS, P., Melt dynamics with MEMENTO —
 Code development and numerical benchmarks, Nuclear Materials and Energy 37 (2023) 101545.
- [10] TSKHAKAYA, D., Implementation of dressed cross-section model into the BIT1 code, Eur. Phys. J. D 77 7 (2023)
- [11] KOMM, M., RATYNSKAIA, S., TOLIAS, P., PODOLNIK, A., Space-charge limited thermionic sheaths in magnetized fusion plasmas, Nucl. Fusion **60** 5 (2020) 054002.
- [12] TOLIAS, P., KOMM, M., RATYNSKAIA, S., PODOLNIK, A., ITER relevant multi-emissive sheaths at normal magnetic field inclination, Nucl. Fusion 63 2 (2023) 026007.
- [13] KPORHA, F., NORDLUND, K., GRANBERG, F., Sputtering of tungsten surfaces by different ion types: A molecular dynamics study, Journal of Nuclear Materials 613 (2025) 155856.
- [14] VON TOUSSAINT, U., PREUSS, R., Modelling of particle-reflection-distributions of rough surfaces, Nuclear Materials and Energy 41 (2024) 101817.
- [15] EKSAEVA, A. et al., Predictive 3D modelling of erosion and deposition in ITER with ERO2.0: from beryllium main wall, tungsten divertor to full-tungsten device, Phys. Scr. **97** 1 (2022) 014001.
- [16] SICCINIO, M. et al., Development of the plasma scenario for EU-DEMO: Status and plans, Fusion Engineering and Design 176 (2022) 113047.
- [17] SUBBA, F., COSTER, D.P., MOSCHENI, M., SICCINIO, M., SOLPS-ITER modeling of divertor scenarios for EU-DEMO, Nucl. Fusion 61 10 (2021) 106013.
- [18] BAUMANN, Ch., Global tungsten erosion and migration modelling for the EU-DEMO with the ERO2.0 code, Nuclear Fusion (2025) Submitted.
- [19] KUMPULAINEN, H.A. et al., Impact of bivariate energy and angular atomic impact spectra on tungsten erosion in JET, Plasma Phys. Control. Fusion 67 5 (2025) 055044.
- [20] YOU, J.H. et al., Divertor of the European DEMO: Engineering and technologies for power exhaust, Fusion Engineering and Design 175 (2022) 113010.

- [21] DARK, J. et al., Modelling neutron damage effects on tritium transport in tungsten, Nucl. Fusion 64 8 (2024) 086026.
- [22] HODILLE, E., 2D tritium retention prediction in the ITER/DEMO actively cooled divertor in the presence of neutron-induced defects, 2025 Submitted to Nuclear Fusion.
- [23] SCHMID, K., SCHWARZ-SELINGER, T., ARREDONDO, R., THEODOROU, A., POMELLA LOBO, T., Implications of T loss in first wall armor and structural materials on T-self-sufficiency in future burning fusion devices, Nucl. Fusion **64** 7 (2024) 076056.
- [24] SCHMID, K., Re-evaluation of the impact of wall retention on Tritium-self-sufficiency in fusion reactors, Nucl. Fusion **65** 2 (2025) 026039.
- [25] BARATTA, I.A. et al., DOLFINx: The next Generation FEniCS Problem Solving Environment, Zenodo (2023).
- [26] MAVIGLIA, F. et al., Integrated design strategy for EU-DEMO first wall protection from plasma transients, Fusion Engineering and Design 177 (2022) 113067.
- [27] CHEN, W., SUGIYAMA, S., SAKAMOTO, Y., MAVIGLIA, F., GERARDIN, J., Evaluation of first wall charged particle heat load considering connection length in EU DEMO: A benchmarking analysis using PFCFlux and APPLE codes, Fusion Engineering and Design **216** (2025) 115124.
- [28] BACHMANN, C. et al., Re-design of EU DEMO with a low aspect ratio, Fusion Engineering and Design **204** (2024) 114518.